Phased-Only Sampled Fiber Bragg Gratings for High-Channel-Count Chromatic Dispersion Compensation

Hongpu Li, *Member, OSA*, Yunlong Sheng, *Member, OSA*, Yao Li, *Member, IEEE*, and Joshua E. Rothenberg, *Member, IEEE, Fellow, OSA*

***Abstract*—Binary and multilevel phase-only sampling functions are proposed for the sampled fiber Bragg gratings (FBGs) with high channel count, which require significantly less refractive-index modulation than that does the sampled grating with amplitude sampling. The design using the new simulated quenching optimization with temperature rescaling results in high channel uniformity and minimum energy in the out-of-band channels. The technique can be applied to the sampled FBGs with very high channel count. A five-channel nonlinearly chirped multilevel phase-only sampled FBG for tunable chromatic dispersion compensation is demonstrated.**

***Index Terms*—Dammann grating, dispersion compensation, fiber Bragg gratings (FBGs), phase mask, wavelength-division multiplexing (WDM).**

I. Introduction

MULTICHANNEL fiber Bragg grating (FBG) naturally attracts great interest in the dense-wavelength-division-multiplexed (DWDM) systems. A single-sampled FBG can show high performance in the operation for filtering or for chromatic disperion compensation simultaneously in multiple channels, which fit to the ITU grid [1]–[9]. The sampled grating was originally proposed for multichannel semiconductor laser [10]. The most straightforward sampling function is a periodic sequence of rectangular functions. In spectral domain, the rectangular sampling function corresponds to a sinc envelope, which modulates the amplitudes of the multiple channels, resulting in a high channel nonuniformity. The sinc sampling [3] can overcome the nonuniformity problem. However, the sinc-sampled FBG fabrication requires a precise control of both amplitude and phase in the grating, which is very difficult in the phase mask side-writing approach. Although the continuous-writing approach [3] can fabricate the sinc sampled FBG, the implementation of the exact sinc sidelobes in each sampling period at precise locations is a significant challenge.

The inherent problem of both rect- and sinc-amplitude sampling is that the regions between two consecutive samples in the fiber are not written with gratings and therefore have no contribution to the grating reflection. This leads to a requirement for an unrealistically high index modulation in the fiber for the sampled FBG with a high channel count N. For the best use of the fiber photosensitity, a method with overwriting the gratings of different central wavelengths in the same length of fiber [8], [9] was proposed. However, exact matching the channel central wavelengths to the ITU grid is a challenge, and the writing time for gratings of high channel count is too long to be acceptable. Buryak *et al.* [4], [20] proposed a multichannel grating design, which uses a summation of equally frequency-spaced single channel gratings with different relative phases. A variational optimization method is used to minimize the required maximum index modulation in order to achieve the theoretical limit of $\sqrt{N}$. The resultant grating contains however fast varying envelop of the index modulation $\Delta n(z)$, which is difficult to implement with the phase mask side-writing technique.

In this paper, we propose the phase-only sampling function, which produces a high channel count and a good channel uniformity, and the phase-only sampled FBG requires the same apodization curve as that for the single-channel FBG. We show that the maximum refractive-index modulation required for a sampled FBG with N channels is $\sqrt{N/\eta}$ times higher than that for the single-channel grating, where η is the diffraction efficiency of the periodic sampling function. In addition, we show that multilevel phase sampling permits an effective suppression of out-of-band channels. We use the new simulated quenching optimization in the design of the phase-only sampling function to achieve much lower cost function value than that obtained from the conventional simulated annealing optimization. The detailed theory, design, optimization, and fabrication processes are described. A multilevel-phase sampled nonlinearly chirped FBG for tunable dispersion compensation [5] is designed and fabricated and demonstrates a good performance.

II. Sampled FBG Theory

The sampled FBG is a grating whose profile is modulated along the fiber by a periodic sampling function $s(z)$. The effec-

Manuscript received January 22, 2003; revised April 17, 2003. This work was done in part while all the authors were with Phaethon Communications.

H. Li was with Phaethon Communications, Inc., Fremont CA 94538-1386 USA. He is now with the Dept. of Electronical and Electeonic Engineering, Shizuoka University, Johoku, Hamamatsu 432-8501, Japan.

Y. Sheng was with Phaethon Communications, Inc., Fremont CA 94538-1386 USA. He is now with Center for Optics, Photonics and Lasers, Department of Physics, Physical Engineering and Optics, University Laval, Sainte-Foy, QC G1K 7P4 Canada (e-mail: dhli@ipc.shizuoka.ac.jp; sheng@phy.ulaval.ca).

Y. Li was with Phaethon Communications, Inc., Fremont CA 94538-1386 USA. He is now with Alliance Fiber Optic Products (AFOP), Sunnyvale, CA 94085 USA.

J. E. Rothenberg was with Phaethon Communications, Inc., Fremont CA 94538-1386 USA. He is now with Northrop Grumman Space Technology, Redondo Beach, CA 90278 USA.

Digital Object Identifier 10.1109/JLT.2003.815505

tive refractive index of a generic sampled FBG can be expressed as

$$n(z) = n_0 + \mathrm{Re}\left\{\left(\frac{\Delta n(z)}{2}\right)\exp\left[i\left(\frac{2\pi z}{\Lambda}+\phi_g(z)\right)\right]s(z)\right\} \quad (1)$$

where n_0 is the average refractive index of the fiber core, z is the position along the grating, and a single-channel seed grating is with the maximum index modulation $\Delta n(z)$, central pitch Λ, and the residual phase $\phi_g(z)$, which describes chirp of the grating. The sampling function also can be chirped in some cases, such as the sampled FBG for compensating the residual dispersion slope [8]. However, only periodic sampling functions are considered in this paper. We express the periodic sampling function $s(z)$ in the Fourier series

$$s(z) = \sum_{-\infty}^{\infty} S_m \exp\left(\frac{i2m\pi z}{P}\right) \quad (2)$$

where S_m is the complex-valued Fourier coefficient. Then, the refractive-index modulation of the sampled FBG is rewritten as

$$\delta n(z) = \sum_{m=-\infty}^{\infty} |S_m| \mathrm{Re}\left\{\left(\frac{\Delta n(z)}{2}\right) \times \exp\left[i\left(\frac{2\pi m z}{P}+\phi_m+\frac{2\pi z}{\Lambda}+\phi_g(z)\right)\right]\right\} \quad (3)$$

where ϕ_m is the phase of S_m. Substituting (3) into the conventional coupled-mode equations and taking into account only two counterpropagating modes for the reflecting FBG, we obtain [12]

$$\begin{aligned}\frac{\partial R_+}{\partial z} &= -iR_- \sum_{m=-\infty}^{\infty} |S_m|\kappa_0 \times \exp\left\{i\left(-\frac{2m\pi z}{P}+\phi_m+2\Delta\beta z-\phi_g(z)\right)\right\} \\ \frac{\partial R_-}{\partial z} &= iR_+ \sum_{m=-\infty}^{m=\infty} |S_m|\kappa_0 \times \exp\left\{-i\left(-\frac{2m\pi z}{P}+\phi_m+2\Delta\beta z-\phi_g(z)\right)\right\}\end{aligned} \quad (4)$$

where $\kappa_0 = \pi\Delta n(z)/(4n_0\Lambda)$ is the coupling coefficient of the seed grating, $\Delta\beta = \pi\cdot(((2n_0)/\lambda)-(1/\Lambda))$ is the detuning, and R_+ and R_- represent the forward- and backward-mode amplitude, respectively. The coupled-mode equation (4) show that the forward and backward modes are coupled by an infinite series of multiple gratings with the same pitch Λ and chirp $\phi_g(z)$ as that of the seed grating. Only the strength of the mth grating is reduced to $|S_m|\kappa_0$. In fact, the number of multiple gratings is equal to the number of the Fourier coefficients $|S_m|$, which are significantly different from zero and can be determined in the sampling function design. Apart from the strength, the reflection spectrum of each of the multiple gratings is identical to that of the seed grating with the central wavelength determined by the phase matching condition

$$2\Delta\beta - \frac{2\pi m}{P} = 0 \quad (5)$$

so that the neighboring channel spacing is $\Delta\beta = \pi/P$. Note that the phase ϕ_m of the Fourier coefficient S_m is independent of z. This constant phase in each component grating does not affect channel performance but provides free parameters useful for optimizing the sampling function [4], [6], [20].

No additional approximation is required in the sampled FBG theory, except the basic assumption in the coupled-mode equations for the slow variation of the mode amplitude envelop, which permits neglecting the second-order derivative in the wave equation. With a further weak grating approximation neglecting the squared local reflectivity, the grating spectrum can be approximated by the Fourier transform of the grating profile. With this approximation, the spectrum of the sampled FBG becomes a convolution between the seed grating spectrum and the Fourier transform of the sampling function, which is a comb function, resulting in multiple identical channels. However, the latter approximation is not required in the sampled FBG theory, in which the seed grating spectrum is computed not with the Fourier transform, but with the coupled-mode equations.

III. Design Sampling Function

When the spectral passband of the seed grating is narrower than the channel spacing and there is no channel overlap, the sampling function is designed in general independently of the seed grating. This approach is valid for the seed gratings with smooth amplitude and phase profile, such as uniform or chirped FBGs. Note that when the seed gratings contain abrupt phase jumps, such as zero-dispersion filter and third-order dispersion compensators, the periodic sampling function approach can fail because of the channel spectrum distortion, as observed in [4], [20].

The figures of merit for the sampling function are

1) equal Fourier coefficient amplitudes $|S_m|$ with $m = 1,\ldots,N$ for a given channel number N;
2) high-channel-count N, which is desirable in many cases;
3) as high as possible values of $|S_m|$, because for a given required strength of the multiple gratings the higher value of $|S_m|$, the lower value of κ_0, and the lower maximum index modulation requirement.

There is an analogy between the periodic sampling function and the spatial diffractive optics element. Designing a sampling function is equivalent to design a spot-array generator in Fourier optics, which is a computer-generated diffractive grating generating a number of equal spaced and equal intensity spots in the far field of diffraction. In this case, the diffracted spot intensities are equal to the squared Fourier coefficients of the diffractive grating. Their sum is referred to as the diffraction efficiency

$$\eta = \sum_{m=1}^{N} |S_m|^2. \quad (6)$$

.

We write the sampling function of period P as

$$s(z) = s_b(z) \otimes \sum_m \delta(z - mP) \quad (7)$$

where $s_b(z)$ is the sampling function in one period and $\otimes$ is the convolution. The sampling period P is determined by the

required neighboring channel spacing, which is, according to (5), $\Delta/\beta = \pi/P$ in wavenumber and is $\Delta\nu = c/2n_gP$ in frequency, where c/n_g is the effective group velocity. Thus, for a sampled FBG at central wavelength 1550 nm and $n_g = 1.45$, the 100-GHz channel spacing corresponds to the sampling period $P \approx 1$ mm. The 50-GHz channel spacing corresponds to $P \approx 2$ mm approximately.

A. Amplitude Sampling Function

The first sampled FBG [2] used an intuitive rectangle sampling function of width z_1 as, $s_b(z) = \mathrm{rect}(z/z_1)$, where z_1 is the grating burst length within the period P. The Fourier transform of $s(z)$ is a comb function with the interval $1/P$ in the "spatial frequency" domain $u = v/(c/n_g)$. The ensemble of channels are modulated by an envelop $(z_1/P)\mathrm{sinc}(uz_1/P)$, which is the Fourier transform of $s_b(z)$. The channels are highly nonuniform. A uniform comb of channels can be generated by a sinc-sampling function [3], $s_b(z) = \sin c(zN/P)$. Now the ensemble of channels are modulated by $(P/N)\mathrm{rect}(uP/N)$ of the width (N/P), in which there are N channels with equal spacing of $1/P$ and equal amplitude.

The main drawback of the rect- and sinc-amplitude modulation sampling function is the low diffraction efficiency: In the sinc sampling, for instance, $|S_m| \propto 1/N$, which reduces the strength of the multiple gratings by a factor of $1/N$. The maximum index modulation in the sampled FBG must be N times higher than that in the single-channel grating. For a high channel counts $N = 40$, this required high index modulation in the fiber can becomes difficult or impossible to achieve, due to the material limit of the maximum achievable photoinduced refractive index change. This inherent problem of the amplitude sampling is due to the absence of grating, which could contribute to the reflection, in the large fraction of the sampling period. The amplitude sampling functions are equivalent to amplitude spatial gratings, which contain large portions of opaque regions and therefore result in low diffraction efficiency. The "unused" portions of the FBG were proposed to be overwritten with additional interleaved sets of amplitude sampling functions and thereby obtain interleaved groups of channels [8].

B. Phase-Only Sampling Function

The phase-only sampling functions have high diffraction efficiencies. The phase-only sampling function is equivalent to the phase-only holograms in the Fourier optics, which do not absorb the incident beam. The theoretical maximum diffraction efficiency is 82% for a binary phase spot generator, and 99%, for a 16-phase-levels grating [21], but only 10% for a binary amplitude grating.

Some authors [4], [14] proposed a linear combination of a set of phase-only functions as the sampling function. Variational analysis was used to optimize different relative phases introduced to the component phase-only functions in order to achieve high diffraction efficiency. The resulting sampling function however is not itself a phase-only function, but includes amplitude modulation, which needs to be implemented in each sampling period (≈1 mm for 100- GHz channel spacing) when writing the FBG. We propose the phase-only sampling function, which does not require additional amplitude apodization in each sampling period (≈1 mm) and is easier to implement with the phase mask side-writing method. The sampling function can be designed with downhill, gradient-descent, and other nonlinear optimization methods. We use the simulated annealing to design the phase-only sampling functions in this paper. Our approach results in high channel count, high channel uniformity, and high diffraction efficiency.

When all the Fourier coefficients have the equal amplitude, we have from (6) with the diffraction efficiency η

$$|S_m| = \sqrt{\frac{\eta}{N}} \tag{8}$$

for $m = 1, \ldots, N$. According to (4), the coupling coefficient for each of the multiple gratings becomes

$$\kappa_m = \kappa_0\sqrt{\frac{\eta}{N}}. \tag{9}$$

Therefore, for a given reflectivity, the maximum index modulation required for the phase-only sampled FBG with N channels is $\sqrt{N/\eta}$ times of that of the seed grating, rather than N times required with sinc-amplitude sampling. For $N = 40$ and $\eta = 0.8$, only seven times higher maximum index modulation is required in the 40-channel phase-only sampled FBG.

C. Dammann Sampling Function

The Dammann grating [15] is a binary phase-only grating, which generates an array of light spots with equal spacing and equal intensity. For implementation of the Dammann sampling FBG, a number of π phase shifts must be inserted within the sampling period. For an FBG of period $\Lambda \approx 0.5$ μm and wavelength $\lambda = 1550$ nm, a π phase shift corresponds to a spatial shift of approximately 250 nm in the FBG, which can be obtained by inserting the same spatial shifts in the phase mask [16]. In our design of Dammann grating, we try to minimize the number of the π phase shifts. That could facilitate the mask fabrication and diminish stitching errors and other errors in the phase mask.

The Dammann sampling function $s_b(z)$ is a binary phase-only function that contains K alternative phase segments of 0 and π (or -1 and 1 in amplitude) of varying segment lengths in each sampling period, as expressed by

$$s_b(z) = \sum_{n=0}^{K} \exp(i\theta_n)\mathrm{rect}\left[\frac{z - \frac{(z_{n+1}-z_n)}{2}}{z_{n+1} - z_n}\right] \tag{10}$$

where $\theta_n = n\pi$ and z_n with $n = 0, 1, \ldots, K$ denote the phase transition point positions. The Fourier coefficients of $s_b(z)$ are given as

$$S_m = \frac{-1}{2im\pi}\sum_{n=0}^{K}(-1)^n\left[\exp(-2i\pi m z_{n+1}) - \exp(-2i\pi m z_n)\right] \quad \text{for } m \neq 0. \tag{11}$$

$$S_0 = \sum_{n=0}^{K}(-1)^n(z_{n+1} - z_n), \quad \text{for } m = 0. \tag{12}$$

When the required number of channels is odd $N = 2M + 1$, designing the Dammann sampling function is to determine a

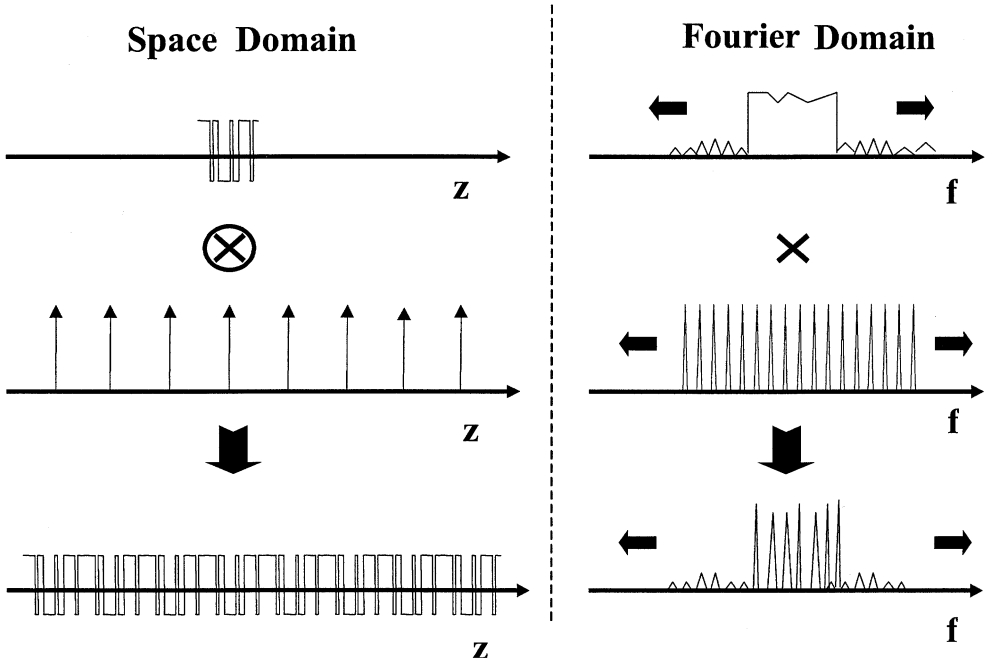

Fig. 1. Fourier analysis of a seven-channel binary-phase-only sampling function.

set of z_n with $n = 1, \ldots, K$, such that a set of $2M$ equation $|S_0|^2 = |S_{\pm 1}|^2; \ldots; |S_0|^2 = |S_{\pm M}|^2$ are satisfied. Usually, one sets the number of unknown transition points equal to number of equations $K = 2M$. However, there are 2^{2M} sets of equations, when altering the sign of each S_m to $+$ or $-$. Using the nonlinear optimization, we can look for a set of solutions z_n that minimizes the cost function, such that the diffraction efficiency $\sum_{m=-M}^{M} |S_m|^2$ is maximum and the differences among $|S_m|^2$ are minimum. In the conventional design of Dammann grating, the period is mirror symmetric with respect to the center of the period, so that the spot array is also symmetric. Then, we have a set of M equations instead of $2M$ equations, and we can determine M unknown transition points in the half period. The physical transition point number in the entire period is still $2M$.

In order to reduce the number of the transition points in the sampled FBG, we give up the symmetry of the sampling function and perform the nonsymmetric grating design with a minimum number of transition points $K < 2M$. In this case, the set of solutions are overdetermined. The nonlinear optimization permits the overdetermined optimal solutions, which minimize the cost function. In the design results shown subsequently, we used $K = 6$ phase transitions for $N = 9$ channels and $K = 22$ for $N = 39$ channels, which are significantly less than $K = 8$ for $N = 9$ and $K = 38$ for $N = 39$ required in the conventional symmetrical Dammann gratings.

However, for even number channels $N = 2M$, we have to still use the transition symmetry of the sampling period such that

$$z_n = z_{n-M} + \frac{P}{2}, \quad \text{for} \quad \frac{P}{2} \le z \le P \tag{13}$$

and

$$\theta_n = \theta_{n-M} + \pi, \quad \text{for} \quad M+1 \le n \le 2M. \tag{14}$$

The property of the Fourier transform ensures removal of all the even diffracted orders and the keeping of only odd orders, resulting in an even number of channels [17], [19]. As the even diffracted orders are absent, the remaining interleaving channel spacing is twice as large as that for odd channel number. Thus, to obtain even channel sampled FBG with 100-GHz channel spacing, for instance, the sampling period should be 2 mm approximately.

D. Simulated Quenching Optimization

Simulated annealing is a recursive Metropolis algorithm to reduce a cost function with a progressively decreasing control parameter called temperature T. The cost function is defined as

$$E(z) = \sum_{-M}^{M} \left[|S_m(z)|^2 - \frac{\eta}{2M+1} \right]^2 \tag{15}$$

where $\boldsymbol{\eta}$ is the target diffraction efficiency. First, an initial solution for a set of transition point positions z_n with $n = 1, \ldots, K$ is chosen randomly. The cost function is evaluated using (11), (12), and (15). Then, each of z_n is shifted randomly with a uniform density of probability. If a move of z_n in the k iteration leads to a decrease of the cost $\Delta E_k = E_k - E_{k-1} \le 0$, the new z_n is accepted. Otherwise, if $\Delta E_k > 0$, the new z_n is still accepted with a probability

$$h(\Delta E_k) = \exp\left(-\frac{\Delta E_k}{T}\right). \tag{16}$$

The simulated annealing is based on an analogy with statistical mechanics. The acceptance probability defined in (16) is such that the Gibbs–Boltzman probability distribution for thermal equilibrium of the ensemble of solutions is maintained before

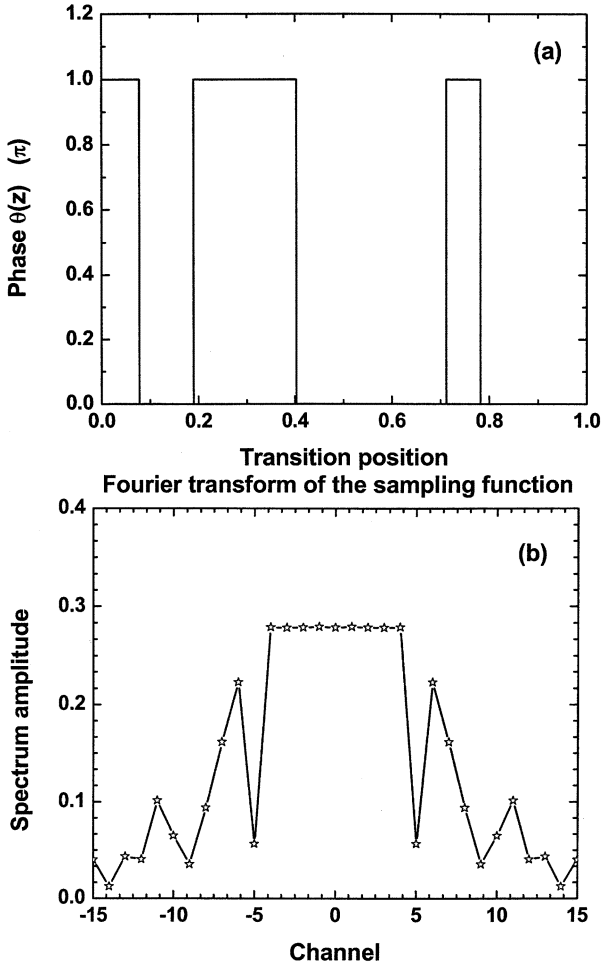

Fig. 2. Nine-channel binary-phase-only sampling function and its Fourier transform.

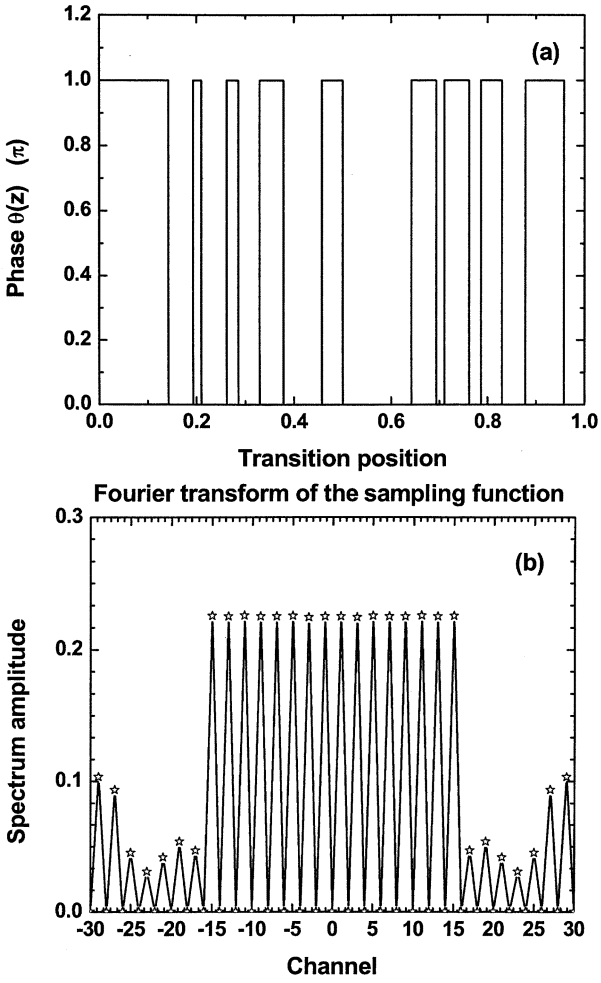

Fig. 3. Sixteen-channel binary-phase-only sampling function and its Fourier transform.

and after the acceptance of the new solution. When the simulated annealing is modeled mathematically as a homogeneous Markov chain, it can be proved that the simulated annealing could lead to a globally optimal solution, provided that the temperature decreases sufficiently slowly and at each temperature a sufficiently large number of the Metropolis steps are executed. In practice, however, the exponential cooling rate

$$T(k) = T_0 \exp\left(-\alpha k^{\frac{Q}{K}}\right) \tag{17}$$

is widely used, where α is a positive constant, k is the number of the Metropolis step, K is the dimension of the space of the parameters to be optimized, and Q is a quenching factor. When K is large, the cooling schedule (17) is too slow with the quenching factor $Q = 1$. Usually one uses $Q = K \gg 1$, which leads to a fast quenching instead of annealing, resulting in a local minimum of the cost function. The difficulty of the simulated annealing is that, in the end of the optimization process when the T is close to zero, the probability $h(\Delta E_k)$ for accepting new uphill transitions $\Delta E_k > 0$ is very small, so that the process can stagnate to a local minimum of the cost function.

In our design, we use the novel simulated quenching with temperature rescaling process [18], in which the T is decreased with a high quenching factor $Q = K$. But at each end of the quenching process, the temperature is rescaled according to the ensemble statistic parameters of the system as

$$T_{\text{rescale}} = \frac{\sigma_{\text{eq}}^2}{(\langle E\rangle_{\text{eq}} - E_e)} \tag{18}$$

where $\langle E\rangle_{\text{eq}}$ and σ_{eq} are the mean and variance of the cost function, respectively, evaluated in the quenching process approximately when the system is close to the frozen state, and E_e is the local minimum cost achieved in the end of a quenching process. The temperature recalling brings the system back from a frozen imperfect state with a local minimum of cost to a dynamic state in a Boltzman heat bath in thermal equilibrium. Our experiments showed [18] that the consecutive new quenching brings the system to a new solution with a lower cost. The quenching and recalling processes continue iteratively until a much lower cost function is achieved.

A variety of designs were completed for the Dammann sampling FBGs. We illustrate the Fourier analysis of a seven-channel binary-phase sampled FBG in Fig. 1. The FBGs of 9, 16, and 39 channels are shown in Figs. 2, 3, and 4, respectively. For convenience, the period of the sampling function is normalized to one, so that all the transition points lie between 0 and 1. The diffraction efficiencies obtained in the

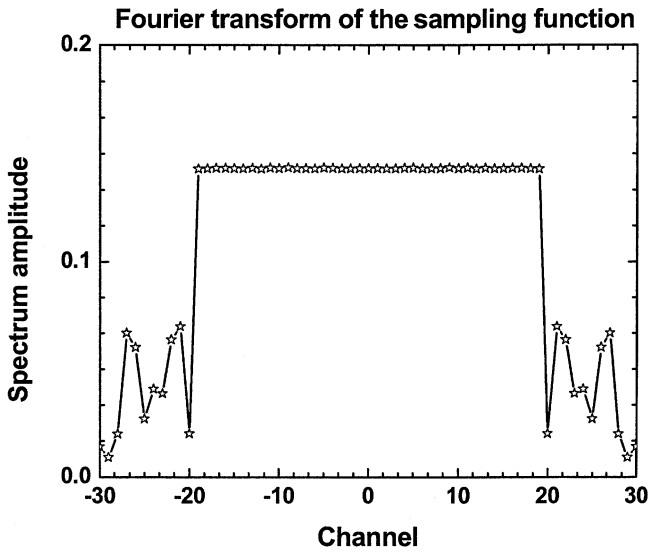

Fig. 4. Thirty-nine-channel binary-phase-only sampling function and its Fourier transform.

TABLE I
BINARY PHASE TRANSITION POINTS FOR 9-, 16-, AND 39-CHANNEL DAMMANN SAMPLING FUNCTIONS

Transition points	9 channel	16 channel	39 channel
Z1	.0777663	0.142331	0.045192
Z2	0.189622	0.193346	0.071555
Z3	0.402680	0.210017	0.099943
Z4	0.712148	0.261666	0.125192
Z5	0.781924	0.286102	0.160475
Z6	1.000000	0.329654	0.191846
Z7		0.378405	0.298697
Z8		0.457695	0.337190
Z9		0.500000	0.417166
Z10		0.642331	0.435823
Z11		0.693346	0.474310
Z12		0.710017	0.510692
Z13		0.761666	0.580630
Z14		0.786102	0.628523
Z15		0.829654	0.639010
Z16		0.878405	0.747023
Z17		0.957695	0.831738
Z18		1.000000	0.849734
Z19			0.875427
Z20			0.907146
Z21			0.953769
Z22			1.000000

optimization with the simulated quenching are 78%, 82%, and 81% for the three designs, respectively. Nonuniformity of the channel intensity in each case is less than 2%. Note that in the 16-channel grating, the alternated channels are suppressed to zero through the entire wavelength span. The phase-transition data of the 9, 16, and 39 channel's designs are given in Table I. To verify the accomplished designs, the required π phase transitions of the Dammann sampling function were inserted into a single-channel FBG. Then, the reflection spectrum of the sampled FBG was computed with the FBG analysis transfer matrix method. The results are shown in Fig. 5. The reflection

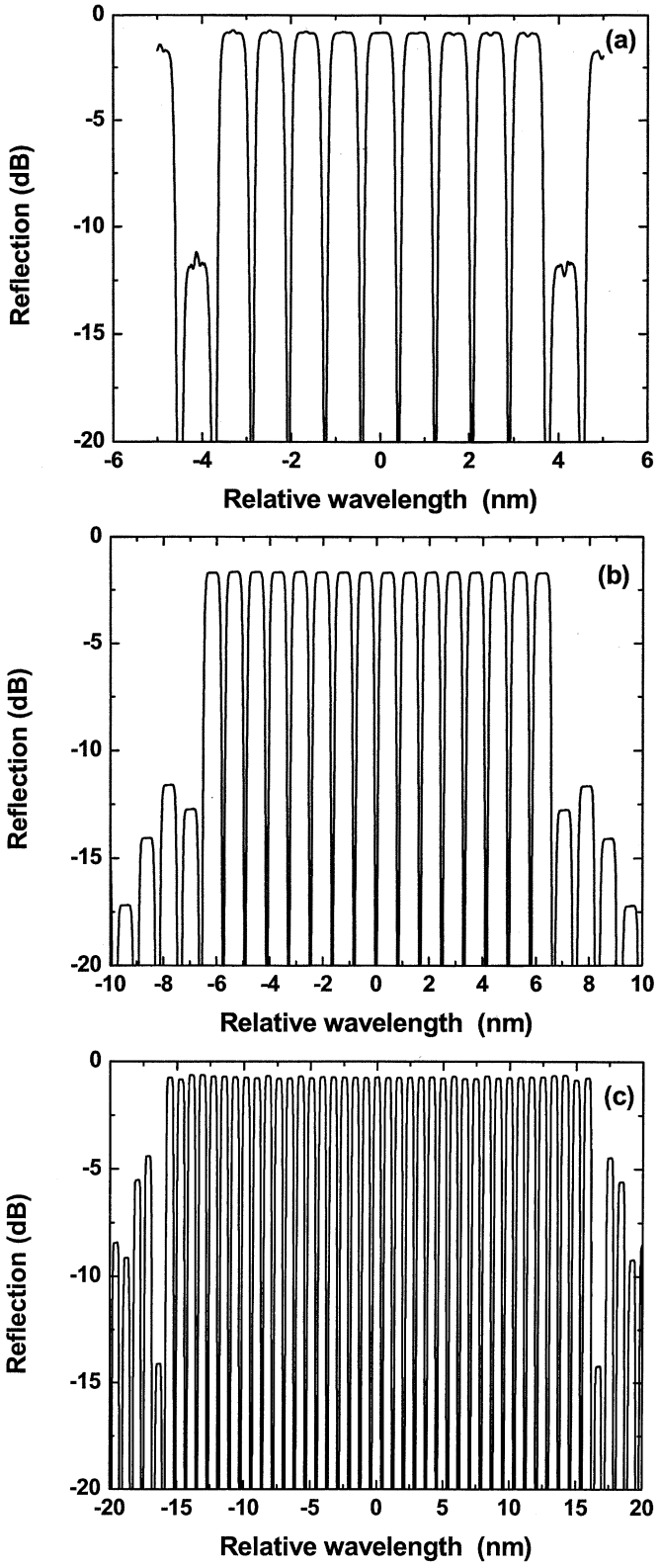

Fig. 5. Calculated reflection spectrum of the Dammann binary-phase-only sampled FBGs for (a) 9 channels, (b) 16 channels, and (c) 39 channels, with 0.8-nm channel spacing.

spectra of these gratings closely agree with what expected for the sampled FBG and with high uniformity over the channels.

The diffraction efficiency of the binary phase Dammann sampling function is typically about 80% [19]. Nearly 20% of the

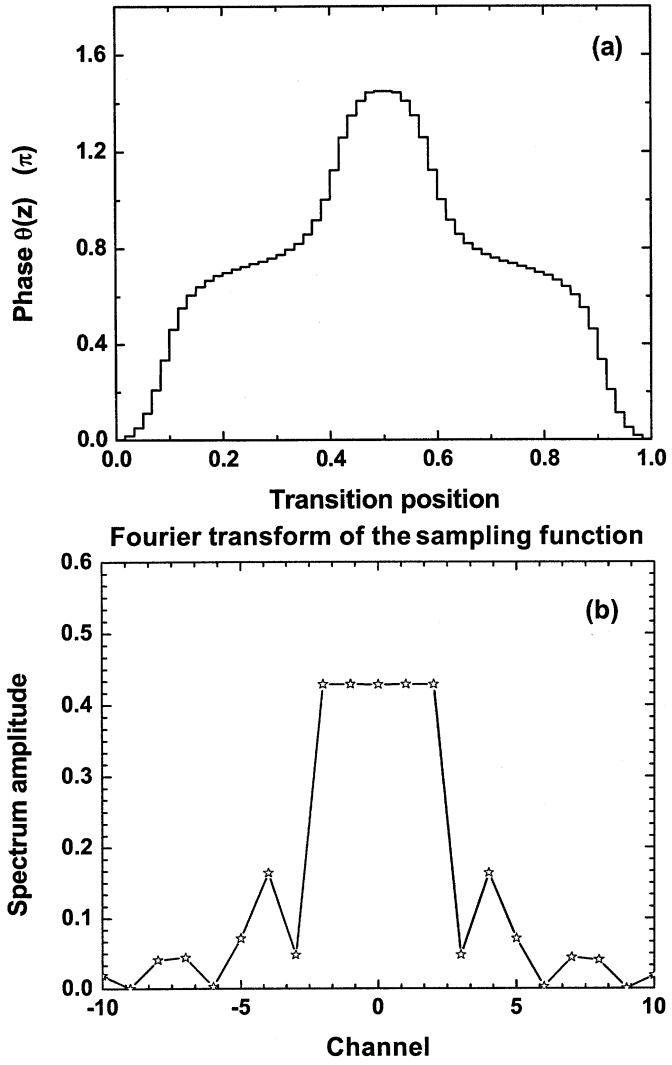

Fig. 6. Five-channel multilevel-phase-only sampling function and its Fourier transform.

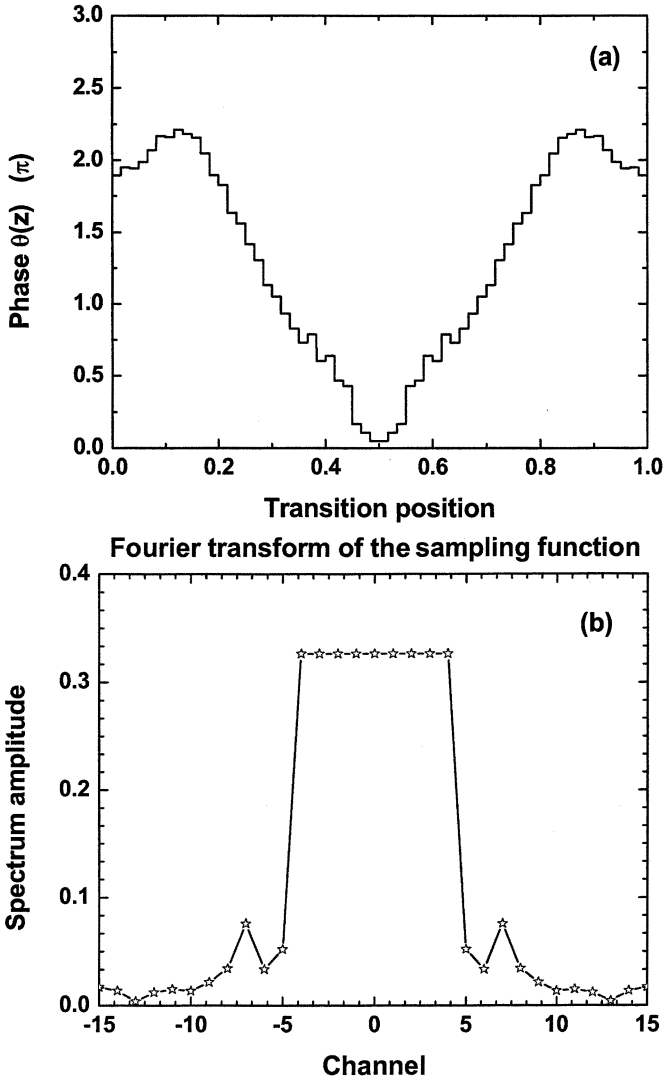

Fig. 7. Nine-channel multilevel-phase-only sampling function and its Fourier transform.

power reflected by the sampled FBG goes to the channels in out-of-band, so that the Dammann sampling can be used only to the applications, which do not require suppression of the out-of-band channels to zero reflectivity.

E. Multilevel Phase Sampling Function

The multilevel phase sampling can achieve much higher diffraction efficiency and higher channel counts than that the Dammann sampling does, so that the out-of-band channels can be minimized. However, the multilevel phase sampling is realizable only when one is able to implement multilevel phase shifts in the phase mask. In the multilevel phase sampling, we let the phase transition points uniformly distributed within the sampling period P. Hence, the sampling function is of

$$S_b(z) = \sum_{n=0}^{K} \exp(i\theta_n) \cdot \mathrm{rect}\left[\frac{z - \frac{(z_{n+1}-z_n)}{2}}{z_{n+1}-z_n}\right] \tag{19}$$

with the equally spaced z_n and the phase shift θ_n in the range $(0, 2\pi)$. Its Fourier transform is

$$S_m = \frac{1}{2im\pi} \sum_{n=0}^{K} \left(-2i\pi mn \frac{P}{K}\right) [\exp(i\theta_{n+1}) - \exp(i\theta_n)], \quad \text{for } m \neq 0. \tag{20}$$

$$S_0 = \left(\frac{P}{K}\right) \cdot \sum_{n=0}^{K} \exp[i\theta_n], \quad \text{for } m = 0. \tag{21}$$

When the number of phase segments K is large enough, both the in-band diffraction efficiency and the channel count can be high. We used the same simulated quenching algorithm as that used for Dammann sampling to the design of the multilevel phase sampling function. The parameters to be optimized here are the set of phases θ_n for $n = 1, \ldots, K$, whose values varies continuously (128 phase levels) within $(0, 2\pi)$. Typical designs for five- and nine-channel sampling functions are shown in Figs. 6 and 7, respectively, where each sampling period was divided into 60 segments. The diffraction efficiency obtained was 92% and

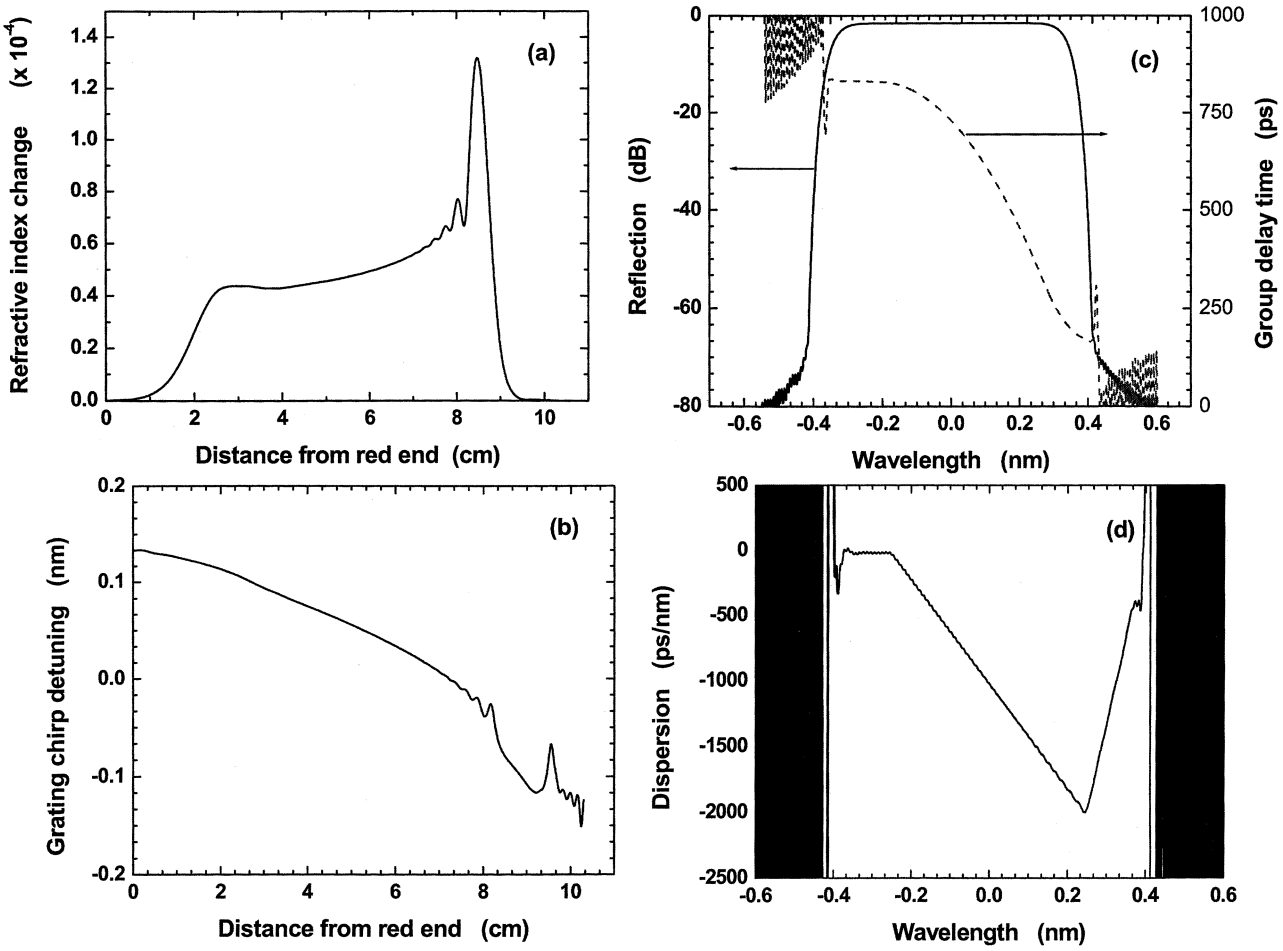

Fig. 8. Synthesized single-channel nonlinearly chirped FBG. (a) Apodization curve. (b) Grating chirp detuning. (c) Reflection and group-delay spectrum. (d) Dispersion spectrum.

96%, respectively. The nonuniformities of the in-band channel intensities were less than 0.1%.

IV. Experimental Results

A five-channel phase-only sampled nonlinearly chirped FBG for tunable dispersion compensation was designed and fabricated. First, a single-channel nonlinearly chirped seed grating was designed using the layer-peeling synthesis algorithm [13]. The grating is designed to have a length of 10.1cm and to provide a quadratic group delay τ as

$$\tau = D_2\Delta\lambda + \frac{1}{2}D_3\Delta\lambda^2 \tag{22}$$

where the second- and third-order dispersion coefficient $D_2 = -1020$ ps/nm and $D_3 = -4000$ ps/nm^2 and $\Delta\lambda$ is the detuning from the central wavelength. The synthesized grating and its calculated reflection spectrum are shown in Fig. 8. Then, we multipled the seed grating by the multiple phase level sampling function shown in Fig. 6 with the period $P \approx 1$ mm. Using the conventional FBG analysis codes, we found that this sampled grating generates five channels with the wavelength spacing of 0.8 nm and with nearly identical reflectivity, group delay, and dispersion spectrum, as shown in Fig. 9. Note that this design method can be easily extended to the sampled FBGs with up to 40 channels covering the whole C or L band in DWDM.

Next, the phase-only sampling function and the nonlinear chirp of the seed grating were encoded into the grating, whose local period becomes

$$\Lambda_M(z) \approx \frac{2}{\Lambda^{-1} + \frac{d\Phi(z)}{dz}\frac{1}{2\pi}} \tag{23}$$

where Λ is the central pitch and $\Phi(z) = \Phi_g(z) + \theta_n(z)$ is the local phase, as defined in (1) and (12). There are two approaches to implement $\Lambda_M(z)$. Ideally, one can change every period of the grating. In this case, the phase mask must be written with the required accuracy and written continuously without stitching. One can also divide the entire grating into a large number of steps. Each step is considered as a uniform grating with the local average period $\Lambda_M(z)$. The latter approach is an extension of the conventional step chirped grating to the sampled and chirped grating. We used the former approach. The phase mask is designed and fabricated with a special "stitch-error-free" lithography tool.

The sampled FBG was written with the side-writing technique. The ultraviolet (UV) source is a 100-mW 244-nm Argon intracavity frequency doubled laser with a beam size about 1 mm. The fiber-to-phase mask spacing was tens of micrometers.

TABLE II
SPECIFICATIONS FOR THE FABRICATED FIVE-CHANNEL NONLINEARLY CHIRPED GRATING

Channel	1	2	3	4	5
Center Wavelength (nm)	1550.511	1551.310	1552.111	1552.912	1553.713
Bandwidth (nm)	0.352	0.350	0.352	0.350	0.352
D2 (ps/nm)	-1130	-1126	-1132	-1148	-1133
D3 (ps/nm^2)	-4963	-5217	-5314	-5304	-5083
Group Delay Ripple P-P (ps)	25	21	23	28	23
Reflectivity Ripple (dB)	0.95	0.78	0.92	0.99	0.99

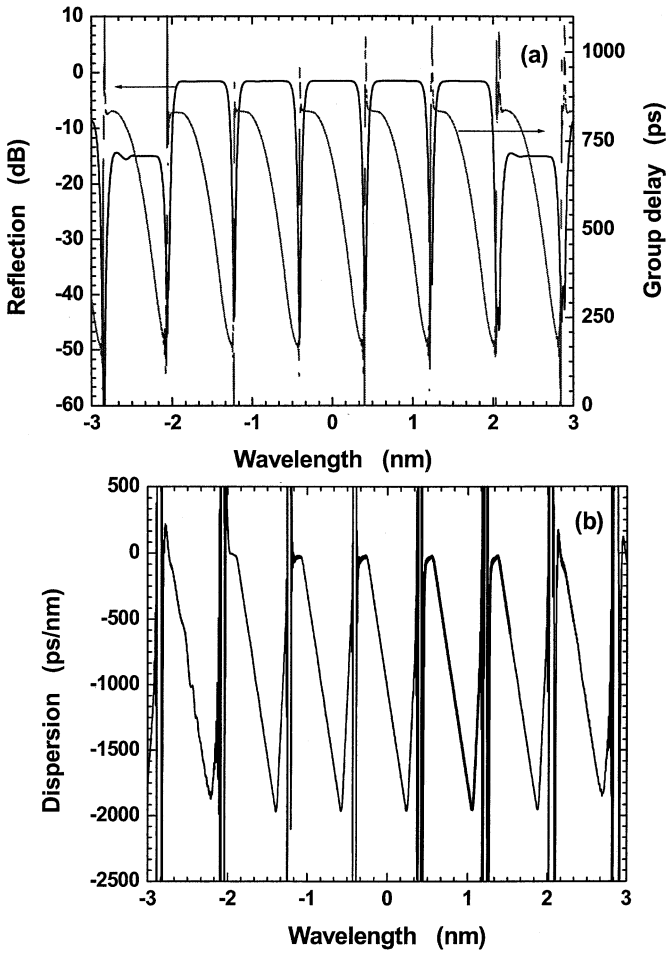

Fig. 9. Design of a five-channel nonlinearly chirped FBG using multilevel phase-only sampling function. (a) Reflection and group-delay spectrum. (b) Dispersion spectrum.

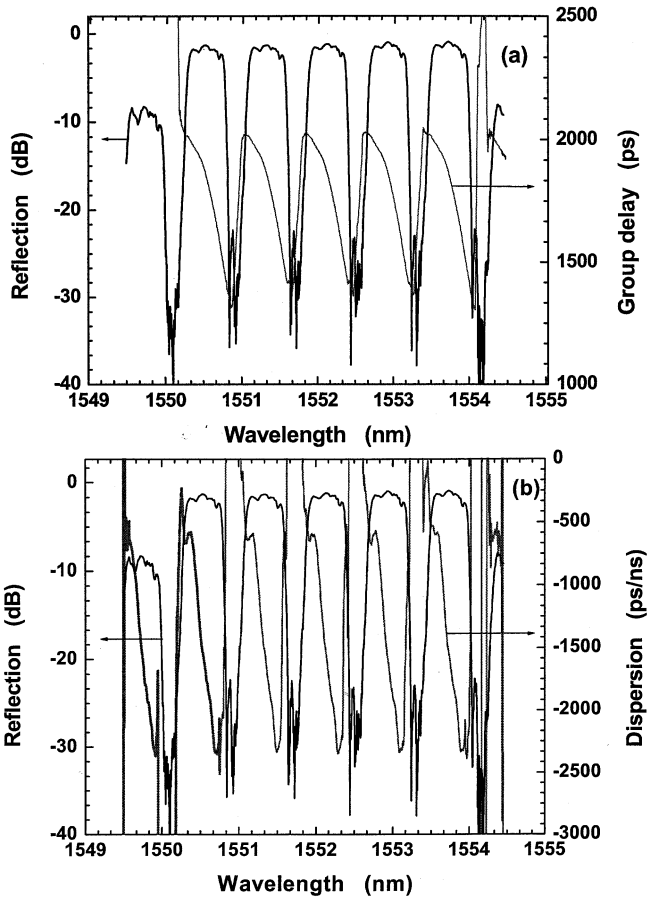

Fig. 10. Measured results of five-channel nonlinearly chirped FBG. (a) Reflection and group-delay spectrum. (b) Dispersion spectrum.

The apodization was controlled by wiggling the phase mask. The phase mask was clamped on a piezo stage, which is a capacitive sensor feedback-controlled device with $+/-1$-nm repeatability and 0.05- nm resolution. Varying the dither amplitude of the piezo stage, while the focused UV beam is scanning along the fiber at a constant speed, changes the fringe visibility along the grating. When the mask is dithered at a half of grating period, for instance, the grating fringes would be erased completely. The dithering amplitude curve was determined according to the required apodization by a sinc fitting.

The measured results on the fabricated FBG are shown in Fig. 10 and are listed in Table II. The time delay curve was measured using a HP86037A chromatic dispersion test system. The grating strength is about 5.2 dB (70% reflectivity). The delay curve is fit by a quadratic curve fitting in each channel. It can be seen that the reflection amplitude ripple for all the five channels are less than 1 dB, and the p–p group-delay ripple is around 25 ps. The experimental results agree with the design data, except the dispersion slope about -5000 ps/ nm^2 is somewhat larger than the expected -4000 ps/ nm^2, and the bandwidth a bit narrower. The channel reflectivity, bandwidth, and dispersion spectrum are fairly uniform over the five channels.

V. CONCLUSION

We have presented the theory for the sampled FBG and demonstrated that a sampled FBG of N channels would require $\sqrt{N/\eta}$ times higher maximum reflective index modulation than that of the single-channel FBG. We propose the phase-only sampling which results in the maximum diffraction efficiency η. We have shown detailed designs for two types of phase-only sampling

functions: binary-phase Dammann sampling and multilevel phase sampling using the simulated quenching optimization with temperature rescaling. We have shown the asymmetric Dammann sampling function design, which requires a minimum number of phase transition points. We have shown that the multilevel phase-only sampling function can maximize the diffraction efficiency and minimize the out-of-band channels energy. We demonstrated experimentally a five-channel multilevel phase sampled nonlinearly chirped FBG for the tunable dispersion compensation. The grating specifications measured for the fabricated FBG agree well with the theoretical design. The design and fabrication techniques can be easily extended to very high channel counts (>45 channels).

REFERENCES

[1] B. Eggleton, P. A. Krug, L. Poladian, and F. Oullette, "Long periodic superstructure Bragg gratings in optical fibers," *Electron. Lett.*, vol. 30, pp. 1620–1622, 1994.

[2] F. Oullette, P. A. Krug, T. Stephens, G. Dhosi, and B. Eggleton, "Broadband and WDM dispersion compensation using chirped sampled fiber Bragg gratings," *Electron. Lett.*, vol. 31, pp. 899–901, 1995.

[3] M. Ibsen, M. K. Durkin, M. J. Cole, and R. I. Laming, "Sinc-sampled fiber Bragg gratings for identical multiple wavelength operation," *IEEE Photon. Technol. Lett.*, vol. 10, pp. 842–844, June 1998.

[4] A. V. Buryak and D. Y. Stepanov, "Novel multi-channel grating devices," in *Proc. Bragg Gratings, Photosensitivity, Poling in Glass Waveguides*, vol. 61, Opt. Soc. Amer., Washington, DC, 2001, Paper BThB3.

[5] K.-M. Feng, J.-X. Cai, V. Grubsky, D. S. Starodubov, M. I. Hayee, S. Lee, X. Jiang, A. E. Willner, and J. Feinberg, "Dynamic dispersion compensation in a 10-Gb/s optical system using novel voltage tuned nonlinearly-chirped fiber Bragg grating," *IEEE Photon. Technol. Lett.*, vol. 11, pp. 373–375, Mar. 1999.

[6] J. E. Rothenberg, H. Li, Y. Li, J. Popelek, Y. Wang, R. B. Wilcox, and J. Zweiback, "Dammann fiber Bragg gratings and phase-only sampling for high channel counts," *IEEE Photon. Technol. Lett.*, vol. 14, pp. 1309–1311, Sept. 2002.

[7] J.-X. Cai, K.-M. Feng, A. E. Willner, V. Grubsky, D. S. Starodubov, and J. Feinberg, "Simultaneous tunable dispersion compensation of many WDM channels using a sampled nonlinear chirped fiber Bragg grating," *IEEE Photon. Technol. Lett.*, vol. 11, pp. 1455–1457, Nov. 1999.

[8] W. H. Loh, F. Q. Zhou, and J. J. Pan, "Sampled fiber grating based-dispersion slope compensator," *IEEE Photon. Technol. Lett.*, vol. 11, pp. 1280–1282, Oct. 1999.

[9] Y. Painchaud, A. Mailoux, H. Chotard, E. Pelletier, and M. Guy, "Multichannel fiber Bragg gratings for dispersion and slope compensation," in *Tech. Dig. Optical Fiber Communication Conf.*, 2002, Paper. THAA5.

[10] V. Jayaraman, Z. M. Chuang, and L. A. Coldren, "Theory, design, and performance of extended tuning semiconductor lasers with sampled gratings," *IEEE J. Quantum Electron.*, vol. 29, pp. 1824–1834, June 1993.

[11] X.-F. Chen, Y. Luo, C.-C. Fan, T. Wu, and S.-Z. Xie, "Analytical Expression of sampled Bragg gratings with chirp in the sampling period and its application in dispersion management design in WDM system," *IEEE Photonics Tech. Lett.*, vol. 12, pp. 1013–1015, Aug. 2000.

[12] A. Yariv and P. Yeh, *Optical Waves in Crystal*. New York: Wiley, 1984.

[13] R. Feced, M. N. Zervas, and M. A. Muriel, "An efficient inverse scattering algorithm for the design of nonuniform fiber Bragg gratings," *IEEE J. Quantum. Eletron.*, vol. 35, pp. 1105–1115, Aug. 1999.

[14] H. Ishii, Y. Tohmori, Y. Yoshikuni, T. Tamamrua, and Y. Kondo, "Multiple-phase-shift super structure grating DBR lasers for broad wavelength tuning," *IEEE Photon. Technol. Lett.*, vol. 5, pp. 613–615, June 1993.

[15] H. Dammann and K. Gortler, "High-efficiency in-line multiple imaging by means of multiple phase holograms," *Opt. Commun.*, vol. 3, pp. 312–315, 1971.

[16] R. Kashyap, *Fiber Bragg Grating*. London, U.K.: Academic, 1999.

[17] D. C. Chu and J. W. Goodman, "Spectrum shaping with parity sequences," *Appl. Opt.*, vol. 11, pp. 1716–1724, 1972.

[18] J.-N. Gillet and Y.Yunglong Sheng, "Iterative simulating quenching for designing irregular-spot-array generators," *Appl. Opt.*, vol. 39, pp. 3456–3465, 2000.

[19] R. L. Morrison, "Symmetries that simplify the design of spot array phase gratings," *J. Opt. Soc. Amer. A.*, vol. 9, pp. 464–471, 1992.

[20] A. V. Buryak, K. Y. Kolossovski, K. Y. Stepanov, and D. Yu, "Optimization of refractive index sampling for multichannel fiber Bragg gratings," *IEEE J. Quantum Eelctronics*, vol. 39, pp. 91–98, Jan. 2003.

[21] G. J. Swanson, "Binary Optics Technology: Theoretical Limits on the Diffractive Efficiency of Multilevel Diffractive Optical Elements," MIT, Tech. Report 914, 1991.

Hongpu Li received the B.S. and M.S. degrees from Huazhong University of Science and Technology, Wuhan, China, in 1985 and 1988, respectively, and the Ph.D. degree from Shizuoka University, Hamamatsu, Japan, in 2000.

From 1988 to 1995, he worked with State Key Laboratory of Laser Technology, Huazhong University of Science and Technology, where he was involved in the fields of optical information process, optical computing, and free-space optical interconnection. From 1996 to 2000. From March 2000 to March 2003, he first was a Postdoctoral Scientist at NEC Research Institute, NJ, a Research Scientist at Phaethon Communication, CA, and then a Postdoctoral Researcher in Laval University, QC, Canada. In April 2003, he joined the Graduate School of Electronic Science and Technology, Shizuoka University, where his current research interest includes nonlinear fiber optics, fiber Bragg grating and its applications in dense-wavelength-division multiplexing, photonic crystal, and some new optical passive devices. He authored or coauthored more than 40 refereed journal papers and held several patents.

Dr. Li is a Member of the Optical Society of America (OSA).

Yunlong Sheng received the B.S. degree from the University of Sciences and Technology of China in 1964 and the M.Sc., Ph.D., and Doctor d'Etat degrees in physics from the Université de Franche-Comté, Besançon, France, in 1980, 1982, and 1986, respectively.

Since 1985, he has joined the Centre for Optics, Photonics and Lasers, University Laval, Sainte-Foy, QC, Canada, where he is now a Full Professor. He has been author and coauthor of more than 180 technical papers, books, and book chapters and has three pending patents. His research interests involve diffractive optics, fiber Bragg gratings, and optical signal processing.

Dr. Sheng is a Member of the Optical Society of America (OSA) and a Fellow of the SPIE-international society for optical engineering.

Yao Li (M'00), photograph and biography not available at the time of publication.

Joshua E. Rothenberg (M'93) received the M.S. and B.S. degrees from the California Institute of Technology, Pasadena, in 1978 and the Ph.D. degree in electrical engineering from Stanford University, Stanford, CA, in 1983, where he was a Fannie and John Hertz Foundation Fellow.

He was formerly Vice President and Chief Scientist of Phaethon Communications, Chief Scientist of the Laser Science and Technology Program at the Lawrence Livermore National Laboratory, and a Research Staff Member at the IBM T.J. Watson Research Center. He is an internationally recognized expert in experimental and theoretical nonlinear optics in fibers, dispersive effects, and propagation. He has also made significant contributions in the fields of ultrafast optics, laser fusion and has contributed more than 150 papers to technical conferences and journals. In addition, he has a number of patents and patents pending in the field of dispersion compensation and fiber Bragg gratings.

Dr. Rothenberg is a Fellow of the Optical Society of America (OSA).